Scientific Journal of Impact Factor (SJIF): 5.71

e-ISSN (O): 2348-4470
p-ISSN (P): 2348-6406

International Journal of Advance Engineering and Research Development

Volume 5, Issue 03, March -2018

# Optical and Theoretical studies on L-Alanine Oxalate: A Nonlinear Optical single crystal for frequency conversion application

K. Deepa[1], S.Arulmani[2], E. Chinnasamy[2], S. Senthil[2], J. Madhavan [1, *]

[1]*Department of Physics, Loyola College, Chennai, India*
[2]*Department of Physics, Government Arts College for Men, Nandanam, Chennai, India*

**ABSTRACT :** *A nonlinear optical L-alanine oxalate (LAO) single crystal was synthesized and successfully grown by slow evaporation technique at room temperature. The Crystal structure of the as grown crystals was determined by single crystal X-ray diffraction analysis and is compared with the powder X-ray diffraction and theoretically stimulated one. The functional groups are identified by Fourier transform infrared spectral analysis and compared with simulated spectrum. The nonlinear optical efficiency of L-alanine oxalate (LAO) was determined from Kurtz Perry powder technique and the efficiency is almost equal to that of standard KDP crystals. Thermal analysis (TG-DTA) reveals the purity of the crystal and the sample is stable up to the melting point. HOMO–LUMO energies and first order molecular hyper polarizability of L-alanine oxalate (LAO) have been evaluated using density functional theory (DFT) employing B3LYP functional and 6-31G (d,p) basis set. Dielectric constant and dielectric loss of L-alanine oxalate (LAO) are measured in the frequency range from 50 Hz to 5 MHz at room temperatures.*

***Key words*:** *Single crystal XRD; FTIR; DFT; NLO; optical studies; hardness studies,*

## I. INTRODUCTION

Semiorganic NLO crystals are expected to possess the advantages of both inorganic and organic materials. 'Semiorganics' are salts in which the typically high optical nonlinearity of a purely organic ion is combined with the favorable mechanical and thermal properties of an inorganic counterion. In semiorganics, polarizable organic molecules are stoichiometrically bound within an inorganic host. Amino acids are interesting materials for NLO applications. Complexes of amino acids with inorganic salts are promising materials for optical second harmonic generation (SHG) as they tend to combine the advantages of the organic amino acid with that of the inorganic salt. In recent years semiorganic crystals have emerged as extremely promising building blocks for NLO materials [1]. L-Histidine is one of the optically active amino acid having an imiadazole side chain with pKa near neutrality [2]. It acts both as a proton donor and proton acceptor. It also acts as a nucleophilic agent [3]. The molecular NLO active crystals have been intensively studied to establish the observed structure-function correlation through the computational modeling of molecules as the origin of the nonlinear optical response in such systems are governed by the electronic polarizability of the electrons at the molecular level [4] as well as the geometrical arrangement of the NLO-chromophores present in the molecular system. The sensitive understanding of the structural and electronic response properties of NLO materials have been provided extensively both experimentally and theoretically using the quantum mechanical density functional theory (DFT) approach by vibrational spectroscopy. The molecular structural properties such as their atomistic level energy, vibrational frequencies, transition moment directions, magnitudes of the normal modes of vibrations etc. can be simulated with great accuracies by theoretical computational methods. Considerable effort has been devoted to understand the vibrational, optical, nonlinear response and electronic structure properties of the molecule- based NLO active organic crystals by the DFT based quantum chemical analysis [5].In this paper, we report on synthesis, growth, and characterization of L-alanine oxalate (LAO) single crystals. The detailed vibrational spectral studies are aided by DFT calculations to elucidate the assignment of the vibrational spectra and the highest occupied molecular orbital (HOMO), lower unoccupied molecular orbital (LUMO) and the first order hyperpolarizability of this compound is examined. FTIR, optical properties, mechanical properties and SHG efficiency of the material are also studied.

## II. EXPERIMENTAL PROCEDURES

Equimolar amount of L-alanine and oxalic acid were dissolved in double distilled water to prepare the aqueous solution of LAO. In deionized water, L-alanine and oxalic acid are allowed to react by the following chemical reaction

$CH_3CHNH_3COOH + H_2C_2O_4 \rightarrow C_5H_9NO_6$

The synthesized salt of LAO was obtained by evaporating the solvent. The supersaturated solution was prepared in accordance with the solubility data. The solvent was allowed to evaporate and numerous tiny crystals were formed at the bottom of the container due to spontaneous nucleation. The transparent and defect free ones among them were chosen as the seeds for growing bulk crystals. Good optical quality crystals of dimension up to 19x3x6 $mm^3$ were harvested after a period of 20−30 days. The photographs of as grown crystals of LAO are shown in Figure.1.

 

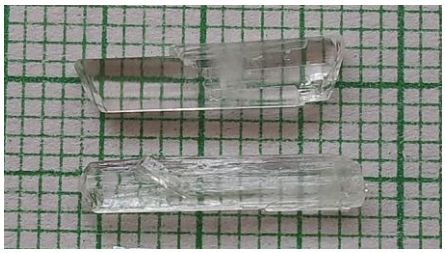

***Figure 1. Photograph of as grown single crystal of LAO***

## III. RESULTS AND DISCUSSION

### 3.1Single crystal XRD

The single crystal XRD was performed to analyze the structure of LAO crystal and the crystallographic parameters. From single crystal XRD study of LAO crystal it was confirmed orthorhombic crystal system having non-centro symmetry with $P2_12_12_1$ space group. The lattice parameters are a=5.590(5) Å, b=7.198(6) Å, c=19.499(3) Å, α=β=γ=90˚ and the volume of the unit cells is found to be 798.3 (2) $Å^3$. Theoretically simulated XRD pattern and experimentally obtained Powder XRD pattern are shown in Figure.2 and Figure.3 respectively. In the title compound, $C_3H_8NO_2^+$,$C_2HO_4^-$, the alanine molecule exists in the cationic form and the oxalic acid molecule in the mono-ionized state Independent part of unit cell contains eight monovalent L-$Al^+$ cations, four $C_2HO_4^-$ anions and ten water molecules. L-alanine cations, oxalate-anions and water molecules are bonded with numerous hydrogen bonds. The alanine molecule exists in the cationic form with a protonated amino group and an uncharged carboxylic acid group. The oxalic acid molecule exists in a mono-ionized state. In the asymmetric unit, the L-alaninium cation and the semi oxalate anion are linked to each other through a N-H…O hydrogen bond. The head-to-tail hydrogen bond, with $O_2$ of the carboxyl group as acceptor, observed among the amino acid molecules in the crystal structure may be described as a zigzag sequence along the $2_1$ screw axis along the direction of the a axis. The alaninium and semi-oxalate ions form alternate columns leading to a layered arrangement parallel to the ac plane and each such layer is interconnected to the other through N-H…O hydrogen bonds. Two short C-O contacts involving the carboxyl oxygen of the alaninium ion [C1…O2(y -1/2 + x, 3/ 2 -y,z) = 2.931 (3) A° and C2…O2(y -1/2 + x, 3/ 2 -y,z) = 2.977 (3) A° ] are also observed in these layers. The slight difference observed in the bond lengths of $C_5$-$O_5$ and $C_5$-$O_6$ in the carboxylate group of the semi-oxalate ion may be attributed to the difference in the strengths of the N-H…O hydrogen bonds in which both $O_5$ and $O_6$ are involved.

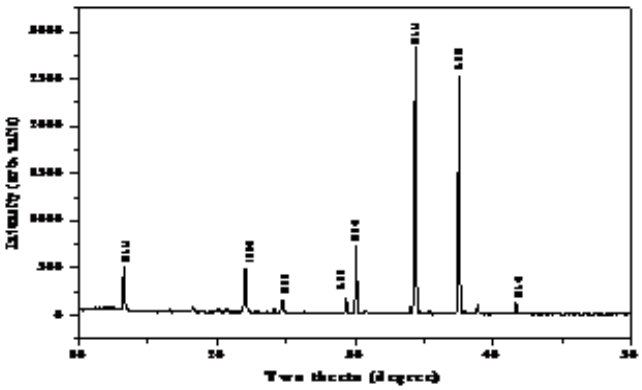

***Figure.2 Experimentally obtained powder XRD pattern of LAO***

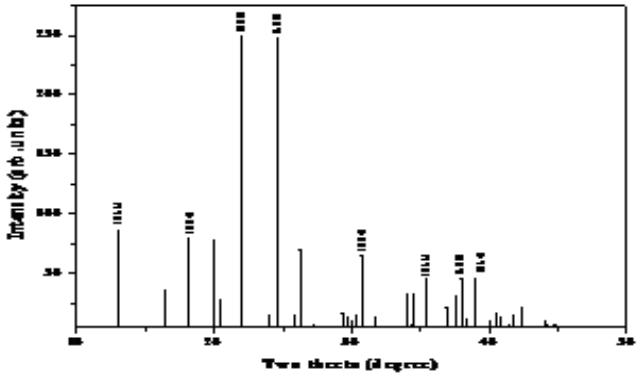

***Figure.3 Theoretically simulated powder XRD pattern of LAO***

 

### 3.2 Computational details

A density functional theory investigation for minimum energy state of LAO molecule is carried out. In order to study the consequence of charge transfer LAO,its electronic property and the optimized structure were computed by using Gaussian 09 package and GaussView [6]. Density functional theory (DFT) methods received much attention since one can simulate the electronic structure of the molecules. Structural optimization were carried in B3LYP/6-31þ G(d,p) level [7,8]. The optimized molecular structure was used to simulate the IR, Raman a hyper polarizability calculations. 1H and 13C NMR isotropic shielding were calculate dousing CDCl3 solvent effect by B3LYP/6- 31þG (d,p) method.

### 3.3 Geometrical structure

As there are two rotamers, viz., the Oxalic and the amino moieties, the molecule can exist in a variety of conformations. A B3LYP/6-31G(d,p) level on full geometry optimization with different spatial dispositions following the standard geometrical parameters, the converged final geometry was the one with all heavy atoms in a plane, with both the hydrogen atoms of the amino group and two of the hydrogen atoms of the methyl group lying out-of-plane. The relevant geometrical parameters like bond length and bond angles have been collected in Tables 1 and 2. It is found from the tables that minimum energy bond length and bond angles are compared with Single crystal XRD parameters. Bond lengths obtained from XRD analysis are smaller than Gaussian values. The differences between this can be attributed to the fact that the theoretical calculations were carried out with isolated molecules in the gaseous phase but the experimental values were based on molecules in the crystalline state [9].

***Table 1. Selected bond length of LAO molecule***

| S.No | Bondlength(A°) | XRD | Gaussian |
|---|---|---|---|
| 1 | $N_1$- $H_{15}$ | 0.8900 | 1.03314 |
| 2. | $N_1$– $H_{11}$ | 0.8900 | 1.02123 |
| 3. | $N_1$– $C_3$ | 1.483(3) | 1.50996 |
| 4. | $C_3$- $H_{14}$ | 0.9600 | 1.09283 |
| 5. | $C_3$– $H_4$ | 0.9600 | 1.09436 |
| 6. | $C_3$ – $C_5$ | 1.522(3) | 1.52647 |
| 7. | $C_5$ – $H_8$ | 0.9600 | 1.09442 |
| 8. | $C_5$ – $H_9$ | 0.9800 | 1.09667 |
| 9. | $C_5$ – $H_7$ | 0.9800 | 1.09471 |
| 10 | $C_6$ – $O_{12}$ | 1.199(2) | 1.36148 |
| 11. | $C_6$ – $O_{10}$ | 1.219(2) | 1.23060 |
| 12 | $C_6$ – $O_{21}$ | 1.297(2) | 1.38068 |
| 13. | $O_{12}$ – $H_{13}$ | 0.8200 | 0.97978 |
| 14. | $C_{17}$ – $O_{21}$ | 1.303(2) | 1.46055 |
| 15. | $C_{17}$ – $O_{20}$ | 1.205(2) | 1.20749 |
| 16. | $C_{17}$ – $C_{16}$ | 1.548(3) | 1.54770 |
| 17. | $C_{16}$ – $O_{18}$ | 1.235(2) | 1.24278 |
| 18. | $C_{16}$ – $O_{19}$ | 1.303(2) | 1.30980 |

***Table2. Selected bond angles of LAO molecule.***

| Bond Angle(degree) | XRD | GAUSSIAN | Bond Angle(degree) | XRD | GAUSSIAN |
|---|---|---|---|---|---|
| $H_{15}$-$N_1$-$H_{11}$ | 109.5 | 110.79229 | $C_{17}$-$C_{16}$-$O_{19}$ | 111.32 | 112.73023 |
| $H_{15}$-$N_1$-$C_3$ | 109.5 | 111.47857 | $O_{20}$-$C_{17}$-$O_{21}$ | 126.65(19) | 117.81369 |
| $H_{11}$-$N_1$-$C_3$ | 109.5 | 112.40390 | $C_{17}$-$O_{21}$-$C_6$ | 120.5 | 121.77214 |
| $H_{14}$-$C_3$-$H_4$ | 109.5 | 108.37728 | $O_{21}$-$C_6$-$O_{12}$ | 109.5 | 111.57625 |
| $H_4$-$C_3$-$C_5$ | 109.6 | 111.88045 | $O_{21}$-$C_6$-$O_{10}$ | 125.65(18) | 125.93896 |
| $H_7$-$C_5$-$H_8$ | 109.5 | 108.24001 | $O_{12}$-$C_6$-$O_{10}$ | 126.65 | 122.09844 |
| $O_{18}$-$C_{16}$-$O_{19}$ | 126.7 | 129.51111 | $H_{13}$-$O_{12}$-$C_6$ | 109.5 | 111.36942 |
| $C_{17}$-$C_{16}$-$O_{18}$ | 118.05 | 117.75787 | $O_{10}$-$C_6$-$O_{12}$ | 121.6 | 120. |
| $C_3$-$C_5$-$H_8$ | 109.5 | 109.5 | $H_{14}$-$C_3$-$C_5$ | 109.65 | 111.46980 |

### 3.4 Hyperpolarizability studies

Interests in organic optoelectronic materials and devices have motivated experimental and theoretical studies of molecular structures with enhanced hyperpolarizabilities. [10]Molecules with electronic asymmetry, or “push-pull” donor- bridge-acceptor electronic framework, have been demonstrated to have large first hyperpolarizabilities (β) [11] Interests in organic optoelectronic materials and devices have motivated experimental and theoretical studies of molecular structures with enhanced hyperpolarizabilities. Molecules with electronic asymmetry, or “push-pull” donor-bridge-acceptor electronic framework, have been demonstrated to have large first hyperpolarizabilities (β). The first static

hyperpolarizability ($\beta_0$) and its related properties ($\beta$ $\alpha_0$ and $\Delta\alpha$ ) have been calculated using B3LYP/6-31G level based on finite field approach. The components of $\beta$ are defined as the coefficients in the Taylor series expansion of the energy in the external electric field.

To calculate the hyperpolarizability, the origin of the Cartesian coordinate system was chosen as the center of mass of the compound [12]. The calculated first hyperpolarizability of LAO is $2.84 \times 10^{-30}$ esu which is 2 times that of KDP. The calculated first hyperpolarizability components are given in Table 4.

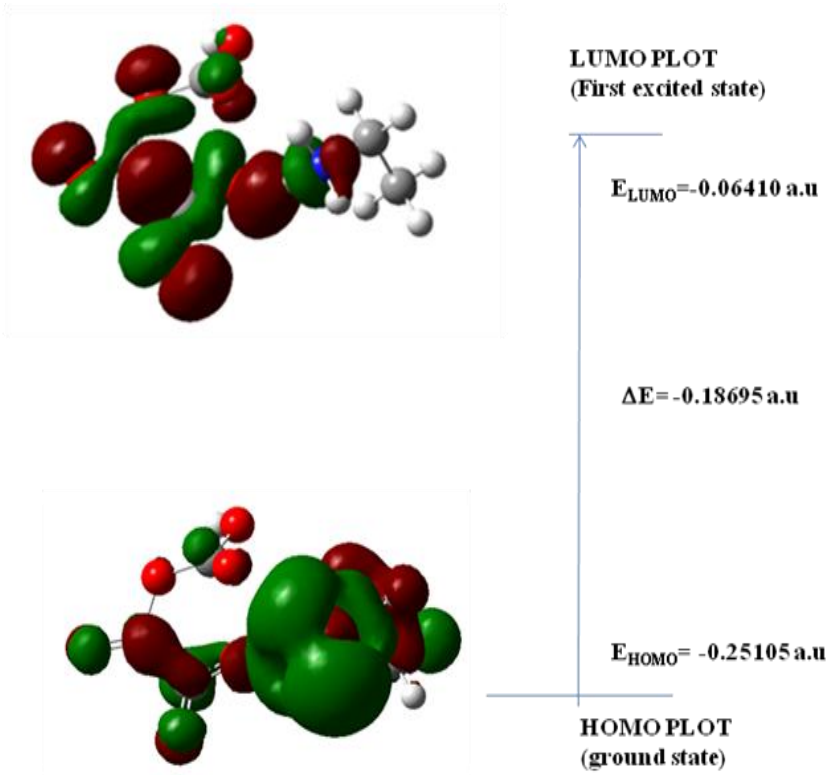


***Figure 4. HOMO – LUMO plot of LAO molecule***

***Table. 3 Hyperpolarizability of LAO in esu***

| | |
|---|---|
| $\beta_{xxx}$ | 123.6388637 |
| $\beta_{xyy}$ | 35.2443193 |
| $\beta_{xzz}$ | 42.7272488 |
| $\beta_{yyy}$ | -3.1986838 |
| $\beta_{yzz}$ | 3.6918875 |
| $\beta_{yxx}$ | -138.9561625 |
| $\beta_{zzz}$ | 22.4016694 |
| $\beta_{zxx}$ | -5.5371442 |
| $\beta_{xyy}$ | 38.7531654 |
| $\beta_{tot(esu)}$ | $2.09921105 \times 10^{-30}$ |

**3.5 HOMO-LOMO analysis**

HOMO and LUMO energies are the important parameters in quantum chemistry. By analyzing the molecular orbital energies one can get how the molecule interacts with other species in the crystal. The frozen orbital approximation and the ground state properties are used to calculate the excitation values. Both the highest occupied molecular orbital (HOMO) and the lowest unoccupied molecular orbital (LUMO) are the main orbital take part in chemical stability. The HOMO represents the ability to donate an electron, LUMO as an electron acceptor represents the ability to obtain an electron. The HOMO and LUMO energy calculated by B3LYP/6-31G(d,p) method are -0.25105a.u and -0.06410a.u respectively and HOMO–LUMO energy gap (B3LYP) = -0.18695a.u. The HOMO is located over the phenyl ring and the carboxylic acid group attached to the phenyl ring. The HOMO →LUMO transition implies an electron density transfer to the carboxylic acid group from the phenyl ring. Moreover, these orbital significantly overlap in their position for LAO Figure.4. The HOMO and LUMO energy gap explains the eventual charge transfer interactions taking place within the molecule. The HOMO-LUMO energy gap of the Molecule is found to be reduced due to the low value of the LUMO and the high value of the HOMO energies which are indicating an enhanced intermolecular charge transfer interactions in the system that leads the molecule as an easily polarizable one. The HOMO→LUMO charge- transfer transition for the molecule is obviously attributed to the $\pi \rightarrow \pi^*$ type contributions. The extended $\pi$-conjugation and charge transfers signify a low energy gap which influences the nonlinear optical properties for LAO.

**3.6 Vibrational analysis**

The LAO molecule has 21 atoms, which possess 57 normal modes of vibrations. All vibrations are active in infrared spectrum. The normal modes of LAO are distributed amongst the symmetry species as 39 in plane and 18 out plane vibrations. Usually the calculated harmonic vibrational wave numbers are higher than the experimental ones, because of the anharmonicity of the incomplete treatment of electron correlation and of the use of finite one-particle basis set. The harmonic frequencies were calculated by B3LYP method using 6-31G (d, p), basis sets experimentally observed and theoretically calculated harmonic vibrational frequencies and their correlations were gathered in Table 5. From the calculations, the computed values are in good agreement with the observed values. The FT-IR spectrum of LAO was recorded using BRUKER IFS-66V spectrometer in the range between 4000 and 500cm$^{-1}$. The resulting spectrum is shown in Figure.5. It coincides well with theoretically simulated FT-IR spectrum shown in Figure.6. Force constant, reduced mass and theoretically simulated IR intensity of the LAO molecule are given in Table 5.

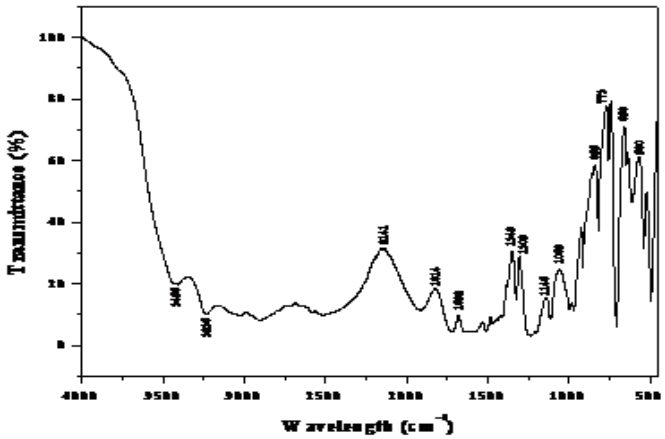

*Figure 5. Experimentally obtained FTIR spectrum of LAO*

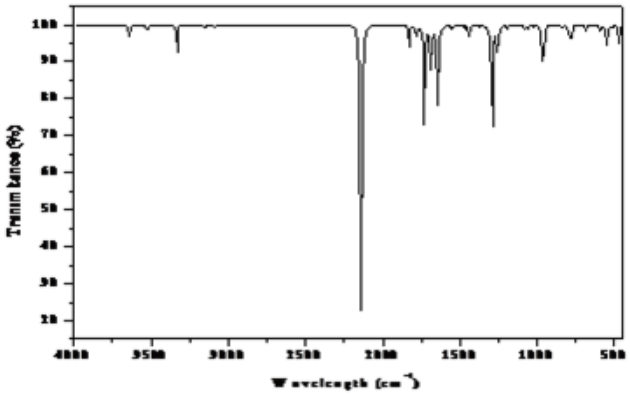

*Figure 6.Theoretically simulated FTIR spectrum of LAO*

**3.6.1 $NH_3$ vibrations**

The zwitterionic form molecules, the $NH_3$ asymmetric and symmetric stretching bands, normally appear in the region 3330 and 3080 cm$^{-1}$, respectively [13]. The strong band observed in IR vibrations at 3054 cm$^{-1}$ corresponds to $NH_3$ asymmetric stretching mode. It has experimental counterpart at 3030 cm$^{-1}$. The red shifting of $NH_3$ stretching wave numbers indicate the formation of intramolecular N–H···O hydrogen Bonding. The short H . . . O distance (H13. . .O12 = 0.9797A˚ ) also supports the existence of N–H···O hydrogen bonding. The $NH_3$ asymmetric deformation vibrations usually appear in the region 1660–1610 cm$^{-1}$ and that of the symmetric deformation in the region 1550–1485 cm$^{-1}$ [14]. In LAO, the $NH_3$ asymmetric deformation vibrations are observed as a very strong band at 1557 cm$^{-1}$ in IR and the symmetric bending modes are observed as a strong band in IR at 1537 cm$^{-1}$.Both the vibrations has its experimental values at1560 and1513 cm$^{-1}$. The $NH_3$ rocking modes appear as a weak band in IR at 962 cm$^{-1}$ and torsions at 39 cm$^{-1}$.

3.6.2 **Carbonyl vibrations**

The C=O stretching vibrations give raise to the characteristic band in IR spectrum, and the intensity of these band can increase owing to the conjugation or formation of hydrogen bonds. The carbonyl stretching vibrations are expected in the region 1760–1730 cm$^{-1}$ [15]. In LAO, there are three carbonyl groups (C6= O10, C16 =O18 and C17= O31). The very

***Table 5. Vibrational Assignments of LAO Molecule***

| Frequency | Experimental frequency ($cm^{-1}$) | Spectroscpic assignment | IR intensity (KM/Mole) | Force constant (mDyne/A°) | Reduced mass(amu) |
|---|---|---|---|---|---|
| 3641.0169 | - | NH st | 71.9725 | 8.3194 | 1.0651 |
| 3525.2361 | - | $NH_2$ asy st | 49.3563 | 7.9127 | 1.0807 |
| 3331.6631 | 3341 | OH st | 177.1868 | 6.9319 | 1.0599 |
| 3158.8209 | - | O-H st | 14.8743 | 1.1057 | 1.1057 |
| 3146.7113 | 3135 | C-H st | 10.6923 | 6.4137 | 1.0994 |
| 3124.3879 | - | $CH_2$ ips | 10.0839 | 6.3190 | 1.0987 |
| 3090.9085 | - | C-H st | 13.8345 | 5.9790 | 1.0622 |
| 3054.0305 | 3030 | $NH_3$asy st | 13.5063 | 5.6998 | 1.0372 |
| 1828.7112 | 1814 | C =O st | 132.2124 | 23.9472 | 12.1539 |
| 1779.6634 | - | C-C st | 59.3880 | 4.3220 | 2.3161 |
| 1731.3753 | 1724 | C =O st | 403.0538 | 4.2672 | 2.4161 |
| 1727.1042 | - | C=C st | 255.0179 | 2.1343 | 1.2144 |
| 1688.1727 | 1692 | C =N st | 270.9033 | 2.1379 | 1.2732 |
| 1644.7270 | 1630 | $CH_2$ ipb | 865.4607 | 2.7875 | 1.7490 |
| 1557.4007 | 1560 | $NH_3$ asy def | 21.3002 | 1.5527 | 1.0865 |
| 1544.6808 | 1538 | C=C st | 15.2743 | 1.4739 | 1.0484 |
| 1537.6173 | 1513 | $NH_3$ sy b | 6.3549 | 1.4493 | 1.0404 |
| 1470.1417 | 1483 | CH ipb | 16.9270 | 1.5320 | 1.2031 |
| 1439.6680 | 1440 | $CH_2$ sci | 64.7713 | 1.6001 | 1.3103 |
| 1373.3448 | 1389 | CH opb | 13.5104 | 1.2841 | 1.1555 |
| 1293.6977 | 1309 | $CH_2$ wag | 877.1389 | 5.8857 | 5.9687 |
| 1287.6724 | - | $NH_3$ tw | 20.9560 | 1.4732 | 1.5080 |
| 1261.8902 | - | OH ipb | 45.4225 | 1.4083 | 1.5010 |
| 1255.8987 | - | C-N st | 158.1905 | 1.9490 | 2.0973 |
| 1191.6827 | 1146 | $CH_2$ roc | 29.4623 | 2.3333 | 2.7887 |
| 1076.3151 | 1102 | OH ipb | 29.5365 | 1.0936 | 1.6023 |
| 1060.6128 | 1069 | PhI | 24.6696 | 0.9601 | 1.4486 |
| 1020.8551 | - | $NH_2$ t | 15.5445 | 0.9602 | 1.5637 |
| 966.1956 | 991 | R asyd | 283.2435 | 6.2753 | 11.4091 |
| 962.8158 | 965 | $NH_3$ roc | 78.3274 | 7.2954 | 13.3571 |
| 880.0578 | 855 | CC | 3.6153 | 1.3124 | 2.8761 |
| 835.2978 | 819 | CH opb | 23.0544 | 0.4539 | 1.1042 |
| 794.7566 | - | R opb | 42.3301 | 4.3985 | 11.8190 |
| 784.3327 | 773 | R berth | 129.7208 | 4.1534 | 11.4592 |
| 686.8864 | 658 | O-H opb | 43.1214 | 3.4271 | 12.3284 |
| 670.7739 | - | NH b | 5.3482 | 2.7267 | 10.2858 |
| 600.6463 | 605 | CN ipd | 25.3086 | 1.9742 | 9.2878 |
| 586.6138 | 580 | C-CO b | 27.0439 | 2.1301 | 10.5061 |
| 548.2281 | 536 | C-C b | 135.7866 | 0.2126 | 1.2008 |
| 514.6009 | 522 | $COO^-$ roc | 14.6141 | 0.2030 | 1.3011 |
| 418.8364 | - | C-C opb | 20.5300 | 0.5787 | 5.5994 |
| 396.8678 | - | R opb | 3.1277 | 0.1898 | 2.0454 |
| 386.4879 | - | C-C b | 11.8996 | 0.6776 | 7.6994 |
| 294.3132 | - | N-H st | 17.3481 | 0.3921 | 7.6828 |
| 247.9294 | - | $NH_2$ t | 2.6787 | 0.0476 | 1.3145 |
| 204.8696 | - | CO opb | 5.7160 | 0.1551 | 6.2715 |
| 166.1278 | - | C-C | 21.7482 | 0.0793 | 4.8777 |
| 128.3344 | - | C-C-N ipb | 8.5613 | 0.0254 | 2.6186 |
| 100.6144 | - | CC ipb | 2.0537 | 0.0398 | 6.6733 |
| 89.6354 | - | R tor | 8.9999 | 0.0250 | 5.2862 |
| 63.3078 | - | $CNH_2$ t | 6.1209 | 0.0088 | 3.7280 |
| 47.9839 | - | R tor | 0.4398 | 0.0051 | 3.7536 |
| 39.9448 | - | $NH_3$ tor | 2.0039 | 0.0076 | 8.0795 |
| 31.7170 | - | CC ben | 0.0499 | 0.0026 | 4.3108 |

strong IR band at 1731 $cm^{-1}$ correspond to C= O stretching modes and coincides with the experimental spectrum at 1724 $cm^{-1}$. When a carbonyl group participates in hydrogen bonding, resonance can occur, which puts a partial negative charge on the oxygen atom accepting the hydrogen bond and a positive charge on the atom donating the hydrogen, the partial

'transfer of allegiance' of the proton enhances resonance and lowers the C= O stretching wave number. The lowering of carbonyl stretching mode is attributed to the fact that the carbonyl group chelate with the other nucleophilic groups, thereby forming both intra and intermolecular hydrogen bonding in the crystal.

### 3.6.3 Hydroxyl vibrations

The OH stretching vibrations are sensitive to hydrogen bonding. The non-hydrogen-bonded or free hydroxyl group absorbs strongly in the 3600–3550 $cm^{-1}$ region, whereas the existence of intermolecular hydrogen bond formation can lower O–H stretching wave number around 3500 $cm^{-1}$ with increase in IR intensity [15]. This theory holds well in the present study. The strong bands observed in IR at 3331 and 3146 $cm^{-1}$ correspond to OH stretching vibrations. The red shifting of OH stretching wave numbers are giving clear evidence for the intermolecular O–H· · ·O hydrogen bonding in the molecule. The in-plane bending of O–H group usually appears as strong bands in the region 1440–1260 $cm^{-1}$ [14]. The strong bands at 1261 and 1076 $cm^{-1}$ in the IR spectrum are assigned to OH in plane bending mode. The O–H out of plane bending vibration gives rise to a strong band in the region 700–600 $cm^{-1}$ [15]. The calculated values of OH group vibrations are in good agreement with the experimental results.

### 3.7 NLO studies

The SHG measuring set up consists of a Q switched Nd:YAG laser of 1064 nm whose beam falls on to a thin section of the material. The second harmonic green light at 532 nm is finally detected using an optical cable attached to a fluorescence spectroscope. For the SHG efficiency measurements, microcrystalline material of KDP was used for comparison. When a laser input of 6.2 mJ was passed through LAO, second harmonic signal of 122 mW is produced and the experimental data confirm a second harmonic efficiency of nearly 1 times that of KDP (124 mW).

### 3.8 Optical properties of LAO

The absorption spectrum plays a vital role in identifying the potential of a NLO material because a given NLO material can be of utility only if it has a wide transparency window without any absorption at the fundamental and second harmonic wavelengths and preferably with the lower limit of the transparency window being well below the 300 nm limits. The spectrum recorded in the range 200 - 1200 nm, (Figure. 7) was obtained with a crystal of thickness 2 mm. From the graph, it is evident that the crystal has a transparency window from 230 nm onwards suggesting the suitability of LAO for SHG of the 1064nm radiation and for other applications in the blue-violet region.

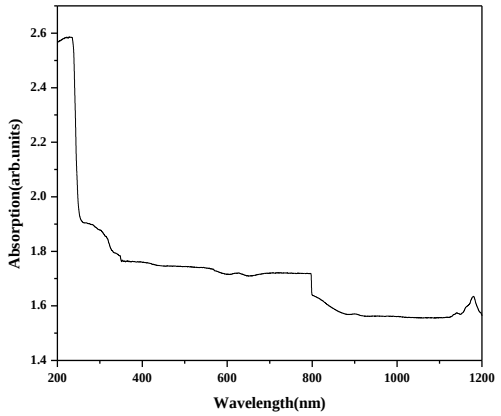


***Figure 7. Optical absorption spectrum of LAO***

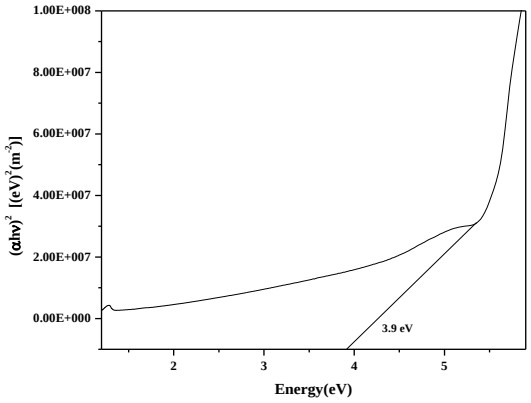


***Figure 8. Energy band gap of LAO***

There is no appreciable absorption of light throughout the visible range, as is the case of all the amino acids. The optical losses in the higher wavelength side could also be reduced by optimizing the growth conditions towards the production of crystals of higher quality. Band gap (figure 8) of LAO is found as 3.9 eV and other linear optical parameters such as extinction coefficient, reflectance, refractive index, complex dielectric constant and optical conductivity are calculated. It is found that the candidate material has low extinction co efficient, low refractive index and high optical conductivity. These suitable values makes the material highly NLO active

**3.9 Microhardness studies**

Vickers hardness test was carried out on a polished sample of LAO using SHIMADZU HMV microhardness tester at room temperature. Several indentations were made for each load at a constant indentation time of 10 s and the Vickers hardness number (Hv) was evaluated for the loads varying from 10 to 50 g. The plot (Figure 9) drawn between the Hv and the applied load indicates that the Hv decreases with increasing load, which is normally attributed to the normal indentation size effect (ISE). In order to know the hardness nature of the material, the work hardening coefficient (n) was determined from the plot between log *p* and log *d* (Figure 10) by the least square fit method. The value of 'n' is found to be 1.73, thus indicating the soft nature of LAO.

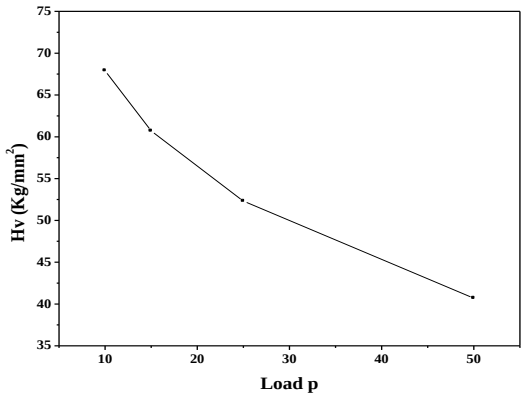


***Figure 9. Vickers hardness number Vs applied load of LAO***

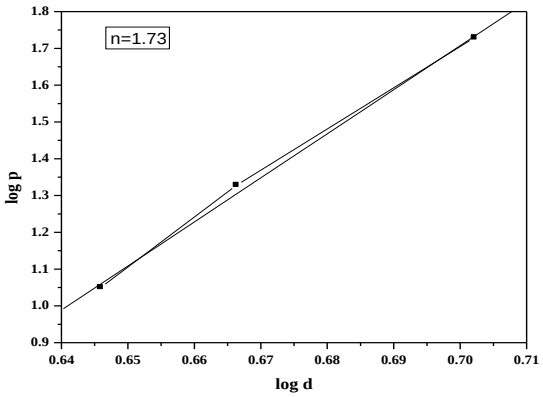


***Figure 10. Log P Vs log d of LAO***

## IV CONCLUSIONS

Good quality Single crystals of L-alanine Oxalate were grown by slow evaporation growth technique at room temperature. The single crystal analysis shows that the crystal belongs to orthorhombic crystal system with $P2_12_12_1$ space group. The powder X-ray diffraction study reveals the structure and crystallinity of the grown crystal land simulated pattern coincides with experimental one with varied intensity patterns. (DFT) computations of LAO molecule calculated by DFT (BLYP) level with 6-31G (d,p) basis set gives the optimized structure. Experimentally obtained bond lengths and bond angles are compared with theoretically calculated one. This property of the material can be used for the electronic applications. Theoretical and experimental IR spectroscopic analysis was carried out and the presence of functional groups in LAO molecule was qualitatively analyzed. HOMO-LUMO analysis reveals the molecular energy gap. The second harmonic generation of the grown crystal was measured and compared with KDP. The gorwn crystal has a transparency window from 230 nm onwards suggesting the suitability of LAO for SHG applications, the optical band gap of LAO is found as 3.9 eV and other linear optical parameters such as extinction coefficient, reflectance, refractive index, complex dielectric constant and optical conductivity are calculated. The value of 'n' is found to be 1.73.

 

**REFERENCES**

[1] Gill AS. and Kalainathan S, Journal of Physics and Chemistry of Solids, 2011; 72: 1002-1007.
[2] Dmitriev V.G, Gurzadyan G.G, Nikogosyan D.N., Hand book of Nonlinear Optical Crystals, 2nd ed., Springer, New York, 1997.
[3] Senthil S, Pari S, Sagayaraj P, Madhavan J, Physica B: Condensed Matter,2009;404: 1655-1660.
[4] Hemalatha A, Deepa K, Venkatesan A, Senthil S, Mechanics, Materials Science & Engineering,2017:9: Doi 10.2412/mmse.85.63.511.
[5] Chinnasamy.E and Senthil. S , American Institute of Physics. 1832 (2017) 100019.
[6] Dennington R, Keith T, Millam J,GaussView 5,SemichemInc, Shawnee Mission, KS, 2009;
[7] Becke D, J. Chem. Phys, 1993;98(7): 5648–5652.
[8] Lee C, Yang W, Parr R.G, Phys.Rev, 1998;B3:7785–789.
[9] Venkatesan .A, Arulmani, S, S.Senthil, Rajasaravanan.M.E, International Journal of Engineering Developemnt and Research.5 (2017) 480-484.
[10] Miller D.A.B, and Chemla D.S, Physical Review B (Condensed Matter), 1987; 35:8113-8125.
[11] Victor Chow K, and Karen C, Denning, Journal of Econometrics, 1993; 58:385-401.
[12] Adant, M .Durpuis , JL Bredas, Int.J.Quantum Chem, 2004;56: 497-507.
[13] Chemla D. S. and Zyss J, "Nonlinear Optical Properties of Organic Molecule and Crystals," Academic press, New York, 1987.
[14] Silverstein R. M, Clayton Bassler G, and Morrill T. C, Spectroscopic Identification of Organic Compounds, 4th edition, John Wiley & Sons, New York, 1981.
[15] Colthup N.B, Daly L.H, Wiberley S.E, Introduction to Infrared and Raman Spectroscopy, Ed 3, Academic Press, New York, 1990; 301-305.

 